

Entangling a polariton with one photon: effect of interactions at the single-particle level

Álvaro Cuevas,^{1,2,*} Blanca Silva,^{1,3,*} Juan Camilo López Carreño,³ Milena de Giorgi,^{1,†}
Carlos Sánchez Muñoz,³ Antonio Fieramosca,¹ Daniel G. Suárez-Forero,¹ Filippo Cardano,⁴ Lorenzo Marrucci,⁴
Vittorianna Tasco,¹ Giorgio Biasiol,⁵ Elena del Valle,³ Lorenzo Dominici,¹ Dario Ballarini,¹
Giuseppe Gigli,¹ Paolo Mataloni,² Fabrice P. Laussy,^{6,3,‡} Fabio Sciarrino,² and Daniele Sanvitto¹

¹*CNR NANOTEC—Institute of Nanotechnology, Via Monteroni, 73100 Lecce, Italy*

²*Dipartimento di Fisica Sapienza University of Rome, Piazzale Aldo Moro, 2, 00185 Rome, Italy*

³*Departamento de Física Teórica de la Materia Condensada,
Universidad Autónoma de Madrid, 28049 Madrid, Spain*

⁴*Università di Napoli Federico II, Napoli, Italy*

⁵*Dipartimento di Fisica, Università degli studi di Trieste, Trieste, Italy.*

⁶*Russian Quantum Center, Novaya 100, 143025 Skolkovo, Moscow Region, Russia*

(Dated: December 17, 2021)

Polaritons are quasi-particles originating from the coupling of light with matter and that demonstrated quantum phenomena at the many-particle mesoscopic level, such as BEC and superfluidity. A highly sought and long-time missing feature of polaritons is a genuine quantum manifestation of their dynamics at the single-particle level. Although they are conceptually perceived as entangled states and theoretical proposals abound for an explicit manifestation of their single-particle properties, so far their behaviour remained fully accountable for by classical and mean-field theories. In this Article, we report the first experimental demonstration of a genuinely-quantum manifestation of microcavity polaritons, by swapping the entanglement between a polariton and an external photon from a photon pair generated by parametric down-conversion. Moreover we demonstrate how interactions manifest at a single polariton level by perturbing the entangled state with a rarefied polariton condensate. Our results open the page of quantum polaritonics and implement the first application of quantum spectroscopy.

Quantum physics presents us with many counter-intuitive features of which entanglement is definitely the most shocking^{1,2}. This thrilling connection between particles endowing them with correlations beyond any local realistic description has an impact on both science (turning everything else into “classical physics”), natural philosophy (with wildly differing interpretations of the theory) and applications (with emerging quantum technologies). It was vividly pictured by Schrödinger with his cat simultaneously alive and dead following its entanglement with a radioactive atom³, and harshly criticized by Einstein as a “spooky action at a distance”⁴. With Bell’s inequalities, philosophy surrendered to physics and its experimental discriminative power to confirm that quantum systems can indeed be entangled⁵. The best control of entanglement is achieved in quantum optics with photon pairs, however the concept has also to be reckoned with in field theory, chemistry, condensed matter and solid state physics^{1,6}. At the meeting point of all these fields lies the concept of “polariton”⁷, itself at the theoretical level an entangled superposition of light with a dipole-carrying medium, of the form $|U/L\rangle = (\alpha|0_a1_b\rangle \pm \beta|1_a0_b\rangle)$, with $|1_a\rangle$ a photon and, depending on the system, $|1_b\rangle$ a phonon, a plasmon, an exciton or even a full atom. The exciton-polariton, that lives in semiconductors, has already championed a reconquest of cold-atoms physics in the solid state, including Bose-Einstein condensation^{8,9}, superfluidity^{10,11}, topological physics¹² and an ever growing list of other exotic quantum macroscopic phases¹³. This wondrous particle

that combines antagonist properties of light (lightweight and highly coherent) and matter (heavy and strongly interacting) also holds great promises for the future of technology by allowing the shift from electronic to optical devices¹⁴ and emerging as the future generations of lasers^{15,16}. As nothing seems out of their reach, one of their major quest is their prospects for quantum-based technologies, as quantum particles akin to photons but with much stronger nonlinearities.

Yet, even in configurations that are expected to provide strong quantum correlations¹⁷, polaritons have so far remained obstinately classically correlated. However useful is their description as a quantum superposition, this is in fact taking advantage of an equivalence with a classical description that is exact in the linear regime and that has enough overlap in the general case as long as one restricts to single-particle observables (first order coherence, power spectrum, intensities, etc.). Stated otherwise, one can describe polaritons with Maxwell equations as resonances in a dielectric medium. This misattribution to quantum physics of effects elegantly described in quantum terms, such as Rabi splitting, but also equally explainable through classical arguments, has long been understood in cavity QED¹⁸. In this way, although the polariton state $\alpha|0_a1_b\rangle + \beta|1_a0_b\rangle$ is genuinely quantum, with α, β complex probability amplitudes, the actual state typically realized in the laboratory is instead a thermal or coherent distributions of such particles that yield, e.g., for the case of coherent excitation, product states $|\alpha\rangle_a |\beta\rangle_b$ ¹⁹. The variables α and β obey the same

equations of motion and evolve identically to quantum probability amplitudes, but they now describe classical amplitudes of coherent fields for the photon (a) and exciton (b), with no trace of entanglement.

This does not invalidate the interest and importance of reaching the genuinely quantum-correlated regime of polaritons^{20–22}. On the contrary, the mental predispositions of a full community to think in quantum terms shows how pressing is to reach this regime. Following decades of sustained efforts from quantum-optimally minded microcavity groups²³ in this direction, the state-of-the-art is the recently reported unambiguous squeezing of the polariton field²⁴. This remains however a weak demonstration of non-classicality (a classical field can be squeezed in all its directions). Much attention has recently been devoted to polariton blockade²⁵, that relies on nonlinearities to oppose the disentangling from an exciting laser and produce some antibunching by favouring low-occupied single particle states. The polariton-polariton interaction however appears to be too weak to reach this regime even in state-of-the-art samples. Much hope was rekindled with the unconventional polariton blockade^{26,27} invoking instead destructive interferences of the paths leading to two-excitation states and thus allowing to get down to the genuinely quantum regime with small nonlinearities. The antibunching is however fast-oscillating and is stronger the smaller the signal, which makes it difficult to observe and indeed all attempts so far have remained thwarted. The race for quantum polaritonics is thus still in its starting blocks.

In this Article, we turn to a new paradigm for bringing quantum polaritons into life. Instead of creating a genuine quantum state from within, e.g., based on strong nonlinearities, we imprint it from outside²⁸. Since photonics is so-far leading in the generation, transfer and manipulation of entanglement, and since photons pair easily to polaritons, this opens an opportunity to realize and explore quantum effects with polaritons with state-of-the-art samples, leaving to technology and growing techniques to provide self-served samples in the future.

In our experiment, the source of entangled photon-pairs is a continuous wave (cw) laser at $\lambda = 405$ nm, down-converted from a Periodically Polarized KTP crystal (PPKTP)²⁹ in order to generate pairs of photons with a bandwidth narrow enough to couple to our microcavity. The latter is composed of front and back Distributed Bragg Reflectors (DBR) with 20 pairs each, confining light, and one $\text{In}_{0.05}\text{Ga}_{0.95}\text{As}$ quantum well (QW), confining excitons. The QW is placed at the antinode of the cavity to maximize their interaction and enter the strong-coupling regime³⁰. The PPKTP is introduced inside a Sagnac interferometer²⁹ (see sketch in Fig. 1) which allows to create polarization entangled photons in a state of the form $|\Psi\rangle = (1/\sqrt{2})(|HV\rangle + e^{i\phi}|VH\rangle)$, where $|H\rangle$ stands for a horizontally polarized photon and $|V\rangle$ for a vertically polarized one. The phase can be controlled in order to create a Bell state $|\Psi^\pm\rangle = 1/\sqrt{2}(|HV\rangle \pm |VH\rangle)$ by placing a liquid crystal in the arm corresponding to

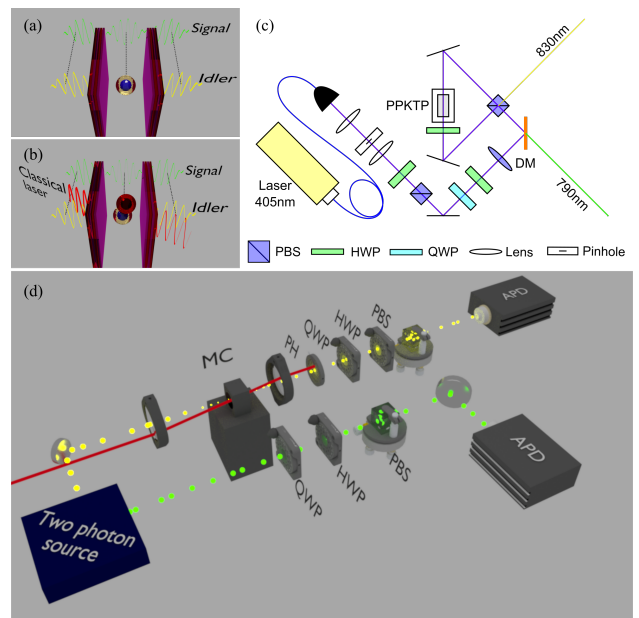


FIG. 1. Sketch of the behaviour inside the microcavity: (a) Linear regime: a single photon (yellow) gets into the microcavity where it becomes a polariton, that is later reconverted into an external photon. When this photon is entangled with another one (green), we show that the entanglement is preserved throughout. (b) Interacting regime: a single photon (yellow) now enters the microcavity along with photons from a classical laser (red). The several polaritons now created inside the microcavity interact. This affects the entanglement of the single-polariton in a way that allows to measure the polariton-polariton interaction. (c) Sketch of the Sagnac interferometric source. (d) Sketch of the setup implementing these configurations.

one of the emitted photons of the interferometer, at the end of which a couple of non-degenerate entangled photons is emitted in different directions: the idler at the wavelength of the polariton resonances ($\lambda \sim 830$ nm), and the signal at higher energies ($\lambda \sim 790$ nm). The high-energy photon is then directed to a standard polarization tomography stage, consisting of a quarter waveplate (QWP) followed by a half waveplate (HWP), a polarizing beamsplitter (PBS) and a single-photon detector (APD). The low-energy photon, instead, is directed towards the microcavity sample. This single photon excites a single polariton in the microcavity, is stored there until its eventual re-emission due to finite polariton lifetime, is retrieved and finally directed to a second tomography stage, equal to the one of the first photon. The coincidence counts deriving from the two single-photon detectors are measured in a 4 ns window using a home-made coincidence detector. By making such measurements for all the combinations of polarization basis for the three polarization bases: circular, vertical and diagonal³¹, we are able to determine whether the photon that transformed into a polariton and back retained the typical

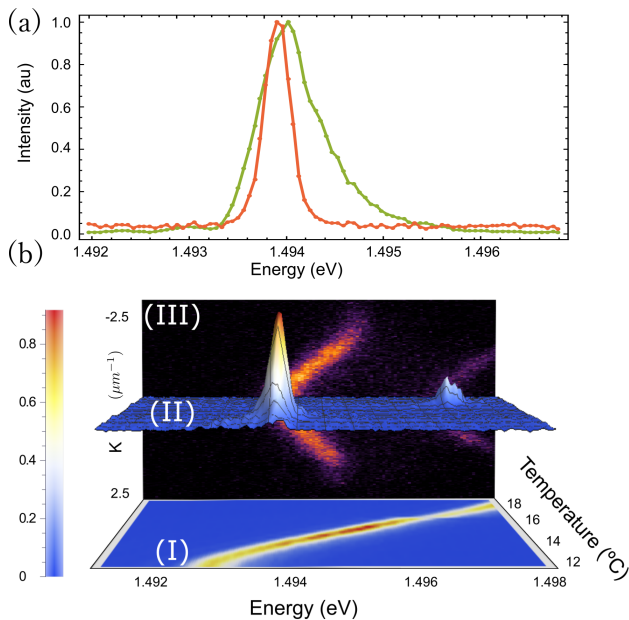


FIG. 2. (a) Green: normalized emission of the PPKTP crystal. Orange: normalized transmission of the emission of the PPKTP crystal through the LPB. (b) Changes on the resonance as a function of the temperature of the two-photon source. I: 2D map of the emission of the crystal outside of the microcavity. II: transmitted intensity as a function of the energy as the temperature varies. Two peaks can be identified that correspond to the resonances with one of the two polariton branches. The color-bar corresponds to both I & II. III: far field of the emission under non-coherent pumping.

nonlocal quantum correlations of a Bell state. If this is the case, this proves that the polariton state that inherited and later passed this information was itself in a genuine one-particle quantum state, and was furthermore entangled with the external photon propagating on the other side of the setup. Namely, we have created the state $|\Psi^\pm\rangle = (1/\sqrt{2})(a_H^\dagger p_V^\dagger \pm a_V^\dagger p_H^\dagger)|0\rangle$ where p_H and p_V are the boson annihilation operators for the horizontally and vertically polarized polaritons and a_H and a_V for the signal photon. For such a bipartite system, entanglement can be quantified through the concurrence, defined in the Methods Section, which is zero for classically correlated or uncorrelated states and gets closer to one the higher the entanglement.

The spectral shape of the idler state is shown in Fig. 2(a). Using single mode laser excitation of the PPKTP crystal, the bandwidth of the entangled photon pairs is reduced to 0.46 nm, which is only 35% wider than the polariton state. Using temperature tuning on the nonlinear crystal we could move the idler resonance from 825 nm to 831 nm. In Fig. 2(b), the effect of the microcavity on the idler state shows that no light is transmitted when the idler is out-of-resonance with the polaritons. This means that no other photons than those that are converted into polaritons are passing through the sample. To study the effect of transferring the entanglement

into the polariton state, we compare the concurrence of the two photons without the microcavity (corresponding to the maximally entangled state) and the one in which the photon is emitted by the microcavity after the idler photon has been converted into a polariton of the Lower Polariton Branch (LPB) with zero momentum ($k = 0$). As can be seen in Fig. 3, the concurrence diminishes from 0.826 in the case of two freely-propagating photons, to 0.806 when one photon is converted into a polariton. Note that the maximum concurrence of the PP-KTP source is limited to 0.826, because of the operation wavelengths needed to interface it with polaritons, where the source can not be fully optimized with the available equipment. Nevertheless, the concurrence is large and remains so in presence of a microcavity on the way. This result is a direct proof that we have generated a single polariton within the microcavity and that it existed there as a quantum state with no classical counterpart. If the single photon was lost in the polariton thermal noise or coupled to a collection of other polariton states, no entanglement would be eventually observed. This transfer of the photon to and from a polariton state has shown to conserve almost entirely the original degree of entanglement. This is encouraging for a future exploitation of quantum polaritonics.

Beyond the preservation of concurrence, we also demonstrated the non-locality between the signal photon and the polariton created by the idler photon. We did so by probing the classical Clauser–Horne–Shimony–Holt (CHSH) inequality³² $S \leq 2$ where:

$$S = |E(a, b) - E(a, b') + E(a', b) + E(a', b')|, \quad (1)$$

with

$$E(x, y) = \frac{C_{++}(x, y) + C_{--}(x, y) - C_{+-}(x, y) - C_{-+}(x, y)}{C_{++}(x, y) + C_{--}(x, y) + C_{+-}(x, y) + C_{-+}(x, y)}, \quad (2)$$

a function of the coincident counts $C_{pq}(x, y)$ between the two measurement ports of our tomography setup, for the photons with polarization $p, q \in \{-, +\}$ in the bases $x = a, a'$ and $y = b, b'$ where $a = -\frac{\pi}{8}$, $a' = \frac{\pi}{8}$, $b = 0$ and $b' = \frac{\pi}{4}$ are the combinations of polarization angles that maximize the Bell's inequality violation. This can be obtained by rotating the tomography HWPs in $a/2$, $a'/2$, $b/2$ and $b'/2$. Figure 4 displays the measured Bell curves, which show the photon coincidences associated to these bipartite polarization measurements, along with the continuous correlated oscillations predicted by the theory. In the optimum configuration, we obtain a value of $S = 2.463 \pm 0.007$ which unambiguously violates the CHSH inequality and proves in this way the non-local character of the photon-polariton system.

The above experimental results clearly demonstrate that although polaritons are quasi-particles in a solid-state system with complex and yet-to-be-fully-characterized interactions with their matrix and other

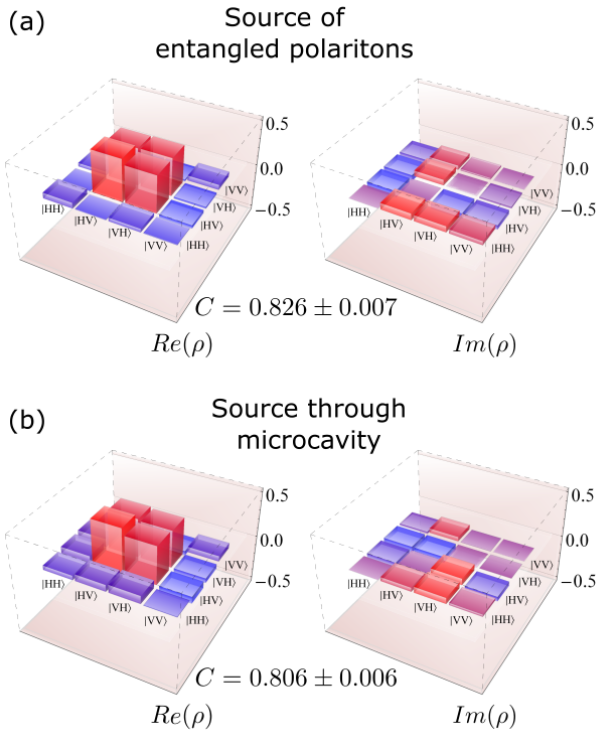


FIG. 3. Tomography measured between the signal (external) and idler (polariton) photons. (a) Real (left) and imaginary (right) components of the density matrix for the source of photon-pairs without the sample. The concurrence of 0.826 is not unity due to the operation wavelength that is not optimal for the source. (b) Real (left) and imaginary (right) components of the density matrix when passing through the microcavity. The concurrence of 0.806 shows that polaritons retain the entanglement.

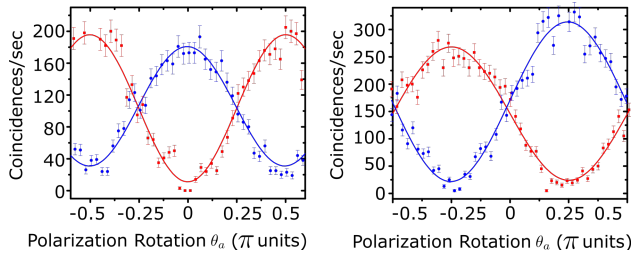


FIG. 4. Coincidences as function of polarization between the external photons and the polaritons. Left: Bell curves for a polarization angle $b = 0$. Right: Bell curves for $b = -\pi/4$. Red squares and blue circles denote the $++$ and $+-$ coincidences, respectively.

polaritons³³, they can be used as quantum bits maintaining almost unvaried their state and do transfer back and forth the quantum state to an external photon field preserving their quantum correlations. This shows in particular that several effects, such as pure dephasing, coupling to phonons, radiative lifetime, etc., are not detrimental to quantum coherence.

The crucial features that we observed in the linear regime can now be transported to the nonlinear regime where several polaritons interact at the few-particle level. To observe such nonlinearities within our available equipment, we repeat the experiment in a non polariton-vacuum configuration. Namely, instead of exciting the sample with one photon of the PPKTP source only, we add the excitation of a classical laser, which is the most common way to excite a microcavity (see sketch in Fig. 1). In this case, the entangled photon is sent on resonance now with the UPB, and the classical laser to the LPB. We have chosen this configuration to avoid any effect of relaxation of the classical source into lower energy states while at the same time keeping the quantum state well distinguishable from the other polaritons. The classical pumping power is changed from having only the vacuum state up to an average of 20 polaritons at any given time, with a density of $10^{-3} \mu\text{m}^{-2}$.

Assuming, first, that these extra polaritons do not interact, they then simply contribute added noise to the PPKTP signal, and some coincidences arise from the detection of uncorrelated photons. This can be corrected provided that we know the average number of such spurious coincidences, which can be easily obtained by repeating the measurement with a spurious temporal delay, which gives the noise due to both the laser, the single polariton and the fake coincidences. While correlations are retrieved in the laboratory by counting coincidences in different polarizations, they are obtained in the theory by computing correlators of the type $\langle a_H^\dagger p_V^\dagger p_V a_H \rangle$ for a_q the signal-photon and p_q the lower-polariton annihilation operators in polarizations $q = V, H$, respectively. In presence of a coherent state $|\alpha\rangle$ in the lower polariton branch following from the coherent drive by the laser¹⁹, the uncorrelated events contribute coincidences of $|\alpha|^2 \langle a_H^\dagger a_H \rangle$. The total coincidences in presence of both the classical laser and the quantum contributions are given by $\langle a_H^\dagger (p_V^\dagger + \alpha)(p_V + \alpha^*) a_H \rangle = \langle a_H^\dagger p_V^\dagger p_V a_H \rangle + |\alpha|^2 \langle a_H^\dagger a_H \rangle + 2\text{Re}(\alpha \langle a_H^\dagger a_H p_V^\dagger \rangle)$. By making the difference of coincidences, with and without temporal delay, we can thus recover the sought correlator $\langle a_H^\dagger p_V^\dagger p_V a_H \rangle$ since one can easily show that $\text{Re}(\alpha \langle a_H^\dagger a_H p_V^\dagger \rangle) = 0$. This allows retrieving the concurrence regardless of the number of non-interacting polaritons (noise) that stem from the classical excitation.

Assuming now that polaritons do interact with each other, the PPKTP signal gets admixed with the polaritons injected by the classical laser. In this case, the polariton entangled to the signal photon becomes dephased from the latter as the former one suffers the effects of its interacting peers while in the microcavity. As a result, once reverted to a photon, the system is found in a degraded situation of entanglement of the quantum state where the polariton that interacted lost its quantum link with the photon that went straight to the detector. This means that when scanning correlations in all the different polarization, the polariton now merely exhibits classical

correlations with the signal photon and the concurrence will consequently vanish. The degree of degradation depends on the strength of the interaction, the number of particles involved and the time spent by the entangled polariton in the microcavity. Its measurement therefore gives access to a lot of information on the system. This mechanism can be simulated theoretically by computing the concurrence for interacting polaritons (see Methods). We modeled pumping and decay with a master equation $\partial_t \rho = i[H, \rho] + \sum_{k=V,H} \frac{\gamma_k}{2} \mathcal{L}_{p_k} \rho + \frac{P}{2} \mathcal{L}_{d^\dagger} \rho$, with H the Hamiltonian of interacting polaritons (spelled out in the Methods) with a Liouvillian in the Lindblad form $\mathcal{L}_c \rho = 2c\rho c^\dagger - c^\dagger c \rho - \rho c^\dagger c$, and $d^\dagger = (a_H^\dagger p_V^\dagger + a_V^\dagger p_H^\dagger)/\sqrt{2}$. The second term of the equation depends on the decays (γ) of both the horizontal (H) and vertical (V) polaritons, and the third one corresponds to the pumping (P) on the sample. The decay rate of the polaritons is independent of their polarization, so that $\gamma_V = \gamma_H = \gamma_{\text{pol}}$. The interaction between polaritons is polarization dependent³⁴, but we assumed here for simplicity that the interaction strength between polaritons with antiparallel spin (U_2) is negligible and assume that the main effect is due to the parallel polaritons interaction (U_1). The computation of the concurrence in this case yields the result shown in Fig. 5 for three values of U_1/γ_{pol} (u) in the range of values usually assumed in the literature²⁵. It shows that the concurrence is fully preserved at small populations but that the interactions ultimately degrade the concurrence until its complete disappearance as it becomes exactly zero. Smaller values of the interaction result in larger populations of polaritons required to spoil the concurrence, which otherwise decays with a similar slope in our simple model. If we now compare this theoretical prediction with the experimental result (data points in Fig. 5 joined by a dashed line to guide the eye), we find a drop of concurrence in excellent qualitative agreement with the model: the concurrence remains constant in a plateau as pumping is increased and then steadily decays toward zero. We could not increase higher the pumping laser in the experiment because of the risk of heating-damage for the sample. Besides, at higher densities, some strong nonlinear effects such as blueshift of the dispersion, due to factors beyond simply polariton-polariton interactions (most likely involving the reservoir) start to dominate. More details on the setup in this case are given in the Methods Section.

The result in Fig. 5 is unambiguous. Photons that were converted into polaritons and interacted with other polaritons injected by a classical laser exhibit a degree of quantum correlation that degrades with the population density of the latter ones. Given that for non-interacting polaritons, the concurrence could be corrected against such polaritons injected by the classical laser, this shows again a direct and explicit manifestation of single-particle effects in the microcavity and directly involving polariton-polariton interactions. The origin of the quantitative departures between the model and the experiment at larger excitations is not yet identified.

This could be due to our neglecting of the opposite-spin small attractive interactions $U_2 \lesssim 0$ or from other similar refinements that remain to be theoretically investigated (e.g., Hopfield fractions, non-local interactions, etc.) or from the onset of more complicated solid-state effects. In spite of these secondary issues, the possibility to observe quantum effects involving interacting polaritons has been demonstrated. Our measurement is the first of its kind and already confirms that polaritons are serious players on the quantum scene through their ability to exhibit nonlinear effects involving a few quanta only. The result further appears to side with the reports (obtained from indirect and classical evidence) of small polariton-polariton interactions^{35,36}. We emphasize here that while such interactions are central to most of their reported phenomenologies¹³ and hold the promise for their future technological applications, there still remain considerable uncertainty on their nature and magnitudes, since they have manifested themselves so far through the involvement of high densities of polaritons. This drags in many other factors, possibly dominant ones, such as heating, phase-space filling, effects from the excitonic reservoir^{37,38}, loss of strong-coupling³⁹ and other hypothetical non-Markovian mechanisms⁴⁰. Possibly, these are also the reasons for the departures also in our quantum case for the highest excitation densities. In our experiment, on the other hand, we have for the first time accessed directly polariton-polariton interactions in a clean environment, at least at the lowest pumpings, where genuine quantum properties and how they are affected by nonlinearities at the few-particle levels are exploited to extract information from the system. Beyond the obvious applications this suggests for quantum gates (routing polaritons in pre-determined landscapes so as to make them interfere⁴¹), this also brings to the laboratory the era of quantum spectroscopy, suggested theoretically by several groups^{28,42-44}. Our experiment is therefore a pioneering demonstration of using quantum-correlated light to access phenomena and information that are out of reach of a classical laser.

I. METHODS

Entanglement for bipartite systems can be quantified unambiguously from the ‘‘concurrence’’, that extracts the amount of non-classical correlations from a so-called detection matrix defined as⁴⁵:

$$\theta_\rho(t, t + \tau) \equiv \begin{pmatrix} \text{HHHH} & \text{HHVH} & \text{HHHV} & \text{HHVV} \\ h.c. & \text{HVVH} & \text{HVHV} & \text{HVVV} \\ h.c. & h.c. & \text{VHHV} & \text{VHVV} \\ h.c. & h.c. & h.c. & \text{VVVV} \end{pmatrix},$$

where it is understood that, e.g., HVHV stands for the correlator $\langle a_H^\dagger(t)(p_V^\dagger p_H)(t + \tau)a_V(t) \rangle$. From the detection matrix we can derive an averaged density matrix

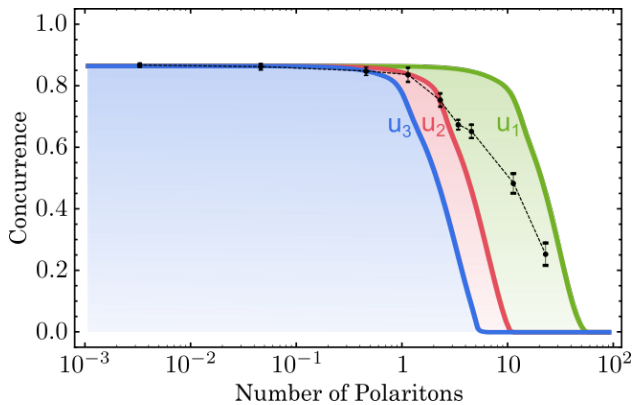


FIG. 5. Concurrence \mathcal{C} between the external photons and the polaritons as a function of the mean number of polaritons present in the sample (horizontal axis) from a classical laser. Each data point is obtained from the 36 measurements of coincidences in all the combinations of polarization (dotted line serves as a guide). Solid lines are theoretical simulations for a simplified model of interacting polarized polaritons for values of $u_1 = 0.01$ (green), $u_2 = 0.05$ (red) and $u_3 = 0.1$ (blue), in excellent qualitative agreement with the observation.

that accounts for the time-integrated observation:

$$\rho_{\text{pol}} = \frac{1}{\mathcal{N}} \int_0^T dt \int_0^T d\tau, \theta(t, t + \tau), \quad (3)$$

where \mathcal{N} is a normalisation constant that makes $\text{Tr}\rho_{\text{pol}} = 1$, and T is the time span in which we measure the correlations. In a steady state situation, t is removed and only the τ dynamics remains, that can bring to the case of perfect same-time coincidences ($\tau = 0$) or registered as such in a small time window. From this matrix, the concurrence is obtained as $\mathcal{C}[\rho] \equiv \max(0, \lambda_1 - \lambda_2 - \lambda_3 - \lambda_4)$ where the λ_i are the eigenvalues of the matrix $\sqrt{\sqrt{\tilde{\rho}}\tilde{\rho}\sqrt{\tilde{\rho}}}$ arranged in decreasing order, with $\tilde{\rho} \equiv (\sigma_y \otimes \sigma_y)\rho^T(\sigma_y \otimes \sigma_y)$.

The dynamics of polarized and interacting polaritons is ruled by the following Hamiltonian (in units of $\hbar = 1$):

$$\begin{aligned} H = & \omega_p \left(p_V^\dagger p_V + p_H^\dagger p_H \right) + 2U_1 p_H^\dagger p_H p_V^\dagger p_V \\ & + \Omega \left(p_V^\dagger + p_V \right) + \frac{U_1 + U_2}{2} \left(p_H^\dagger p_H^\dagger p_H p_H + p_V^\dagger p_V^\dagger p_V p_V \right) \\ & - \frac{U_1 - U_2}{2} \left(p_H^\dagger p_H^\dagger p_V p_V + p_V^\dagger p_V^\dagger p_H p_H \right), \quad (4) \end{aligned}$$

where ω_p is the free polariton energy, Ω is the intensity of a laser driving coherently the polaritons with vertical polarization and U_1 , (U_2) is the interaction strength between polaritons with parallel (antiparallel) spins, respectively. Typically, the polariton interaction is strongly anisotropic, with $|U_1| \gg |U_2|$. For simplicity and since we did not undertake a comprehensive study of the polarization of the driving laser, we have assumed here $U_2 = 0$. The concurrence as defined above computed from $\theta_\rho(\tau = 0)$ for the steady state density matrix for the Hamiltonian (4) supplemented with free-energy for the a and b

photon and ruled by the master equation given in the text yields the concurrence shown in Fig. 5.

II. SETUP

The experiment consist in four different parts: photon generation, signal-photon tomography stage, polariton source and polariton tomography stage. The first part consists of a Sagnac interferometer excited with a single-mode diode laser at 405nm and a pumping power of 6.5 mW and bandwidth FWHM < 5 pm. Its power selection is achieved by fixing a half-wave plate (HWP) before a polarizing beam splitter (PBS), and the horizontal output polarization is again rotated in a desired arbitrary polarization before a dichronic mirror (DM). In order to increase the efficiency of the PPKTP, a lens is introduced to focalize the diode right on the crystal. The second and the fourth sections of the setup are used for the tomography measurement. The idler photon goes through the polariton source, which consists on a cryostat at 20 K and a pressure of 100 mbar. The single-photon is focused on the surface of the microcavity and the emitted photons are recollected with a second lens sending them directly to the fourth stage (the idler's tomography stage). In the experiment measuring nonlinear effects, an additional laser is sent to the microcavity at a particular angle. The transmitted photons given by the laser are covered with a diaphragm (pin-hole, PH) at the Fourier plane of the recollection lens. The entanglement measurement takes place in the tomography analysis⁴⁶. In our case, we apply a hypercomplete tomography by projecting the bipartite state onto a combination set of three bases: logical ($|HVHV\rangle$ & $|V\rangle$), diagonal ($|+\rangle = |HVHV\rangle + |V\rangle$ & $|-\rangle = |HVHV\rangle - |V\rangle$), and circular ($|R\rangle = |HVHV\rangle + i|V\rangle$ & $|L\rangle = |HVHV\rangle - i|V\rangle$). Each local projection is done by applying a rotation in a QWP and a HWP, followed by a PBS as polarization filter (see Fig 1). Finally, the remaining photons belonging to the qubit of both the signal and the idler are coupled to a single-mode optical fiber (SMF), connected to an avalanche photo-detector (APD). The reconstruction of the state sees the relative coincident count events (CC) among all the mentioned projections during the desired integration time. In that way, we measure the state by projecting many copies of the same.

III. ACKNOWLEDGEMENTS

This work was supported by the ERC-Starting Grants i) 3D-QUEST (3D-Quantum Integrated Optical Simulation; grant agreement no. 307783, <http://www.3dquest.eu>) and ii) POLAFLOW (grant agreement no. 308136). It was also partially supported by PhD Chilean Scholarships CONICYT, “Becas Chile” and by the Spanish MINECO under contract FIS2015-64951-R (CLAQUE).

Authors declare no financial competing interest.

- * Both authors contributed equally to this work
 † milena.degiorgi@nanotec.it
 ‡ fabrice.laussy@gmail.com
- ¹ Horodecki, R., Horodecki, P., Horodecki, M. & Horodecki, K. Quantum entanglement. *Rev. Mod. Phys.* **81**, 865 (2009). URL doi:10.1103/RevModPhys.81.865.
 - ² Selleri, F. *Quantum Paradoxes and Physical Reality* (Springer Netherlands, 1990).
 - ³ Schrödinger, E. Discussion of probability relations between separated systems. *Proc. Cambridge Phil. Soc.* **31**, 555 (1935). URL doi:10.1017/S0305004100013554.
 - ⁴ Einstein, A., Podolsky, B. & Rosen, N. Can quantum-mechanical description of physical reality be considered complete? *Phys. Rev.* **47**, 777 (1935). URL doi:10.1103/PhysRev.47.777.
 - ⁵ Aspect, A., Grangier, P. & Roger, G. Experimental tests of realistic local theories via Bell's theorem. *Phys. Rev. Lett.* **47**, 460 (1981). URL doi:10.1103/PhysRevLett.47.460. ASP1.
 - ⁶ Pan, J.-W. *et al.* Multiphoton entanglement and interferometry. *Rev. Mod. Phys.* **84**, 777 (2012). URL doi:10.1103/RevModPhys.84.777.
 - ⁷ Kavokin, A., Baumberg, J. J., Malpuech, G. & Laussy, F. P. *Microcavities* (Oxford University Press, 2011), 2 edn.
 - ⁸ Kasprzak, J. *et al.* Bose–Einstein condensation of exciton polaritons. *Nature* **443**, 409 (2006). URL doi:10.1038/nature05131.
 - ⁹ Christopoulos, S. *et al.* Room-temperature polariton lasing in semiconductor microcavities. *Phys. Rev. Lett.* **98**, 126405 (2007). URL doi:10.1103/PhysRevLett.98.126405.
 - ¹⁰ Amo, A. *et al.* Collective fluid dynamics of a polariton condensate in a semiconductor microcavity. *Nature* **457**, 291 (2009). URL doi:10.1038/nature07640.
 - ¹¹ Amo, A. *et al.* Superfluidity of polaritons in semiconductor microcavities. *Nat. Phys.* **5**, 805 (2009). URL doi:10.1038/nphys1364.
 - ¹² Karzig, T., Bardyn, C.-E., Lindner, N. H. & Refael, G. Topological polaritons. *Phys. Rev. X* **5**, 031001 (2015). URL doi:10.1103/PhysRevX.5.031001.
 - ¹³ Carusotto, I. & Ciuti, C. Quantum fluids of light. *Rev. Mod. Phys.* **85**, 299 (2013). URL doi:10.1103/RevModPhys.85.299.
 - ¹⁴ Ballarini, D. *et al.* All-optical polariton transistor. *Nat. Comm.* **4**, 1778 (2013). URL doi:10.1038/ncomms2734.
 - ¹⁵ Schneider, C. *et al.* An electrically pumped polariton laser. *Nature* **497**, 348 (2013). URL doi:10.1038/nature12036.
 - ¹⁶ Kim, S. *et al.* Coherent polariton laser. *Phys. Rev. X* **6**, 011026 (2016). URL doi:10.1103/PhysRevX.6.011026.
 - ¹⁷ Ardizzone, V. *et al.* Bunching visibility of optical parametric emission in a semiconductor microcavity. *Phys. Rev. B* **86** (2012). URL doi:10.1103/PhysRevB.86.041301.
 - ¹⁸ Zhu, Y. *et al.* Vacuum Rabi splitting as a feature of linear-dispersion theory: Analysis and experimental observations. *Phys. Rev. Lett.* **64**, 2499 (1990). URL doi:10.1103/PhysRevLett.64.2499.
 - ¹⁹ Dominici, L. *et al.* Ultrafast control and Rabi oscillations of polaritons. *Phys. Rev. Lett.* **113**, 226401 (2014). URL doi:10.1103/PhysRevLett.113.226401.
 - ²⁰ Ciuti, C. Branch-entangled polariton pairs in planar microcavities and photonic wires. *Phys. Rev. B* **69**, 245304 (2004). URL doi:10.1103/PhysRevB.69.245304.
 - ²¹ Savasta, S., Stefano, O. D., Savona, V. & Langbein, W. Quantum complementarity of microcavity polaritons. *Phys. Rev. Lett.* **94**, 246401 (2005). URL doi:10.1103/PhysRevLett.94.246401. PEN1.2.
 - ²² Demirchyan, S., Chestnov, I., Alodjants, A., Glazov, M. & Kavokin, A. Qubits based on polariton rabi oscillators. *Phys. Rev. Lett.* **112**, 196403 (2014). URL doi:10.1103/PhysRevLett.112.196403.
 - ²³ Karr, J. P., Baas, A., Houdré, R. & Jacobino, E. Squeezing in semiconductor microcavities in the strong-coupling regime. *Phys. Rev. A* **69**, R031802 (2004).
 - ²⁴ Boulier, T. *et al.* Polariton-generated intensity squeezing in semiconductor micropillars. *Nat. Comm.* **5**, 3260 (2014). URL doi:10.1038/ncomms4260.
 - ²⁵ Verger, A., Ciuti, C. & Carusotto, I. Polariton quantum blockade in a photonic dot. *Phys. Rev. B* **73**, 193306 (2006). URL doi:10.1103/PhysRevB.73.193306.
 - ²⁶ Liew, T. C. H. & Savona, V. Single photons from coupled quantum modes. *Phys. Rev. Lett.* **104**, 183601 (2010). URL doi:10.1103/PhysRevLett.104.183601.
 - ²⁷ Bamba, M., İmamoğlu, A., Carusotto, I. & Ciuti, C. Origin of strong photon antibunching in weakly nonlinear photonic molecules. *Phys. Rev. A* **83**, 021802(R) (2011). URL doi:10.1103/PhysRevA.83.021802.
 - ²⁸ López Carreño, J. C., Sánchez Muñoz, C., Sanvitto, D., del Valle, E. & Laussy, F. P. Exciting polaritons with quantum light. *Phys. Rev. Lett.* **115**, 196402 (2015). URL doi:10.1103/PhysRevLett.115.196402.
 - ²⁹ Fedrizzi, A., Herbst, T., Poppe, A., Jennewein, T. & Zeilinger, A. A wavelength-tunable fiber-coupled source of narrowband entangled photons. *Opt. Express* **15**, 15377 (2007). URL doi:10.1364/OE.15.015377.
 - ³⁰ Weisbuch, C., Nishioka, M., Ishikawa, A. & Arakawa, Y. Observation of the coupled exciton-photon mode splitting in a semiconductor quantum microcavity. *Phys. Rev. Lett.* **69**, 3314 (1992). URL doi:10.1103/PhysRevLett.69.3314.
 - ³¹ James, D. F. V., Kwiat, P. G., Munro, W. J. & White, A. G. Measurement of qubits. *Phys. Rev. A* **64**, 52312 (2001). URL doi:10.1103/PhysRevA.64.052312.
 - ³² Clauser, J. F., Horne, M. A., Shimony, A. & Holt, R. A. Proposed experiment to test local hidden-variable theories. *Phys. Rev. Lett.* **23**, 880 (1969). URL doi:10.1103/PhysRevLett.23.880.
 - ³³ Deveaud, B. Polariton interactions in semiconductor microcavities. *C. R. Physique* (2016). URL doi:10.1016/j.crhy.2016.05.004.
 - ³⁴ Deng, H., Haug, H. & Yamamoto, Y. Exciton-polariton Bose–Einstein condensation. *Rev. Mod. Phys.* **82**, 1489 (2010). URL doi:10.1103/RevModPhys.82.1489.
 - ³⁵ Rossbach, G. *et al.* Impact of saturation on the polariton renormalization in iii-nitride based planar microcavities. *Phys. Rev. B* **88**, 165312 (2013). URL doi:10.1103/PhysRevB.88.165312.

- ³⁶ Trichet, A. *et al.* Long-range correlations in a 97% excitonic one-dimensional polariton condensate. *Phys. Rev. B* **88**, 121407(R) (2013). URL doi:10.1103/PhysRevB.88.121407.
- ³⁷ Ferrier, L. *et al.* Interactions in confined polariton condensates. *Phys. Rev. Lett.* **106**, 126401 (2011). URL doi:10.1103/PhysRevLett.106.126401.
- ³⁸ Christmann, G. *et al.* Polariton ring condensates and sunflower ripples in an expanding quantum liquid. *Phys. Rev. B* **85**, 235303 (2012). URL doi:10.1103/PhysRevB.85.235303.
- ³⁹ Houdré, R. *et al.* Saturation of the strong-coupling regime in a semiconductor microcavity: Free-carrier bleaching of cavity polaritons. *Phys. Rev. B* **52**, 7810 (1995). URL doi:10.1103/PhysRevB.52.7810.
- ⁴⁰ Dominici, L. *et al.* Real-space collapse of a polariton condensate. *Nat. Comm.* **6**, 8993 (2015). URL doi:10.1038/ncomms9993.
- ⁴¹ Sturm, C. *et al.* All-optical phase modulation in a cavity-polariton Mach–Zehnder interferometer. *Nat. Comm.* **5**, 3278 (2014). URL doi:10.1038/ncomms4278.
- ⁴² Kira, M. & Koch, S. W. Quantum-optical spectroscopy of semiconductors. *Phys. Rev. A* **73**, 013813 (2006). URL doi:10.1103/PhysRevA.73.013813.
- ⁴³ Aßmann, M. & Bayer, M. Nonlinearity sensing via photon-statistics excitation spectroscopy. *Phys. Rev. A* **84**, 053806 (2011). URL doi:10.1103/PhysRevA.84.053806.
- ⁴⁴ Mukamel, S. & Dorfman, K. E. Nonlinear fluctuations and dissipation in matter revealed by quantum light. *Phys. Rev. A* **91**, 053844 (2015). URL doi:10.1103/PhysRevA.91.053844.
- ⁴⁵ del Valle, E. Distilling one, two and entangled pairs of photons from a quantum dot with cavity QED effects and spectral filtering. *New J. Phys.* **15**, 025019 (2013). URL doi:10.1088/1367-2630/15/2/025019.
- ⁴⁶ Altepeter, J., Jeffrey, E. & Kwiat, P. G. Photonic state tomography. *Advances in Atomic, Molecular, and Optical Physics* **52**, 105 (2005). URL doi:10.1016/S1049-250X(05)52003-2.